Ninth International Conference on CFD in the Minerals and Process Industries
CSIRO, Melbourne, Australia
10-12 December 2012

EULERIAN-LAGRANGIAN MODELLING WITH STOCHASTIC APPROACH FOR DROPLET-DROPLET COLLISIONS

S. K. PAWAR[1], J. T. PADDING[1]*, N. G. DEEN[1], J. A. M. KUIPERS[1], A. JONGSMA[2], and F. INNINGS[2]

[1]Multiphase Reactors Group, Department of Chemical Engineering and Chemistry,
Eindhoven University of technology , P.O. Box 513, 5600 MB Eindhoven, The Netherlands
[2] Tetra Pak CPS, Heerenveen, The Netherlands
*Corresponding author, E-mail address: J.T.Padding@tue.nl; Tel: (+31) 40 247 3674;Fax: (+31) 40 247 5873

ABSTRACT

In recent years, there has been growing interest to use computational fluid dynamics (CFD) for exploring droplet-particles interaction under the turbulent flow of air inside spray dryer systems. The final goal is to predict the dried solid particle size and mass flux distributions under the conditions of collision, coalescence and agglomeration of the droplets and particles. The coarse-grained simulation tool will be used to design more efficient spray dryers that can produce higher throughputs.

We are developing an Euler-Lagrange model with stochastic treatment of collision, coalescence and agglomeration of droplet-droplet, droplet-particle, and particle-particle combinations in the spray dryer. In this approach, the gas phase is treated as continuum solved by an Eulerian equation and the solid phase is treated as a dispersed phase solved by a Lagrangian equation, with conventional gas-solid coupling. Inside the spray chamber, turbulent gas flow has an effect on the droplet-particle interactions. To take this into consideration we use a sub-grid scale turbulence (SGS) model. In the spray dryer process, the number density of droplets at the nozzle is more than 10^{11} m^{-3}, which is why we employ a Direct Simulation Monte Carlo (DSMC) stochastic approach. In traditional DSMC the system volume is divided into cells and particles collide within a single cell.

In this paper we study collisions in a spray of fine water droplets. To avoid lattice artifacts in our work we use a spherical searching scope, in which one droplet searches for another during a droplet time step. Droplet collisions under turbulent flow are calculated on the basis of a collision probability based on droplet concentration and relative velocity. Depending on values of characteristic dimensionless numbers, outcomes of the collisions are assumed to fall in one post-collision regime or another. In this paper we present the model and first validating steps.

NOMENCLATURE

$\mathbf{u}_g$	Gas velocity	m/s
p	Pressure	kg/(m s^2)
V_{cell}	Volume of the cell	m^3
$\mathbf{v}_i$	Velocity of the i^{th} droplet	m/s
V_i	Volume of the droplet	m^3
d_i	Diameter of the droplet	m
m_i	Mass of droplet i	kg
$\mathbf{F}_{g,i}$	Gravity force	kg m/s^2
$\mathbf{F}_{d,i}$	Drag force	kg m/s^2
$\mathbf{F}_{p,i}$	Pressure force	kg m/s^2
f_i	Collision frequency	1/s
n_i	Number of real droplets represented by i	–
L_i	Mean free path of droplet i	m
Δt_i	Time step for the droplet	s
P_{ij}	Collision probability between i and j in droplet time step Δt_i	-
$R_{s,i}$	Collision searching scope of droplet i	m
N_i	The total number of all representative droplets in the searching scope of droplet *i*	-
$\mathbf{S}_p$	Source term that couples the gas to the dispersed phase	kg/(m^2s^2)
ρ_g	Gas density	kg/m^3
ε_g	Gas porosity	-
$\bar{\bar{\tau}}_g$	Shear stress	kg/(m s^2)
μ_e	Effective viscosity	kg/(m s)
β_i	Drag coefficient for droplet i	kg/(s m^3)
σ	Surface tension	kg/s^2
ρ_d	Droplets density	kg/m^3

INTRODUCTION

Spray drying is an essential unit operation for production of powders from liquid slurry. This technology is widely used in different industries such as the chemical industry, the pharmaceuticals industry, the food industry etc (Woo et al., 2010). Normally, a spray dryer comes at the end of the processing line, as it is an important step to control the final product quality. It has some advantages, such as rapid

drying rates, a wide range of operating temperatures and short residence times (Gianfrancesco et al., 2008).

In recent years, computational fluid dynamics (CFD) has been increasingly applied to explore the spray dryer process. CFD simulations are often used because measurements of airflow, temperature, particle size and humidity inside the drying chamber are very difficult and expensive to obtain in large-scale dryers. However, most works reported in the literature do not consider particle interactions in their simulation. Nowadays, the growing interest to use CFD in predicting the final particle size has led to extensive developments of new techniques that can give insights into droplet–droplet, droplet-particle and particle-particle interactions.

Regarding particle-particle interactions, Goldschmidt et al. (2003) have investigated spray granulation, including experimental studies focusing on each granulation mechanism, techniques for modelling granulation and assessment of granule properties such as structure and strength. Verdurmen et al. (2004) have reported an attempt to simulate the entire agglomeration process. However, a better understanding of particle agglomeration is needed to translate this to industrial operating guidelines. In the literature, little existing work is available that spatially addresses the agglomeration in a spray dryers.

Regarding droplet-droplet interaction, our objective in this paper is to develop a simulation tool that can provide the droplet size distribution for a highly turbulent gas flow section of a large-scale spray dryer. Note that at this stage drying of the droplets has not yet been implemented. The same method to detect collisions between droplets can be applied to wet and dry particles as well as droplets, but in this paper we will focus on droplets. These results ought to be used as boundary conditions for more coarse-grained simulations.

NUMERICAL MODELLING

To model the top section of a spray drier, the following general assumptions were made:

- The turbulent flow involves a gas carrier phase, droplets and particles.
- Encounters between dispersed elements are treated stochastically through encounter rules based on local concentration, relative velocities, and element sizes.
- Droplets are assumed to have a spherical shape in between collisions.

Continuous phase

In this model, we compute the Navier-Stokes equations for the gas phase and Newtonian equations for the motion of the individual droplets, with conventional two-way coupling for the momentum exchange between the gas and discrete phase. For the gas phase, we write the equation of conservation of mass and momentum:

$$\frac{\partial}{\partial t}(\rho_g \varepsilon_g) + \nabla \cdot (\rho_g \varepsilon_g \mathbf{u}_g) = 0 \tag{1}$$

$$\frac{\partial}{\partial t}(\rho_g \varepsilon_g \mathbf{u}_g) + \nabla \cdot (\rho_g \varepsilon_g \mathbf{u}_g \mathbf{u}_g) = -\varepsilon_g \nabla p - \nabla \cdot (\varepsilon_g \bar{\boldsymbol{\tau}}_g) - \mathbf{S}_p + \rho_g \varepsilon_g \mathbf{g} \tag{2}$$

Where, $\mathbf{u}_g$, ρ_g and p are the gas velocity, density and pressure, respectively, and $\mathbf{g}$ the acceleration due to gravity. $\boldsymbol{\tau}_g$ is the viscous stress tensor, in which the turbulent eddy viscosity is calculated from a sub-grid scale stress model, as described in (Vreman et al., 2004). $\mathbf{S}_p$ is a source term that couples the gas to the dispersed phase. It is defined as:

$$\mathbf{S}_p = \frac{1}{V_{cell}} \int_{V_{cell}} \sum_{i=1}^{N} n_i \frac{V_i \beta_i}{1 - \varepsilon_g} (\mathbf{u}_g - \mathbf{v}_i) \delta(\mathbf{r} - \mathbf{r}_i) dV \tag{3}$$

Here v_i is the velocity of a representative droplets with index i, V_i is its volume, n_i the number of real droplets it represents, and V_{cell} the volume of the Eulerian grid cell. The distribution-function δ distributes the reaction force of the droplets acting on the gas phase to the velocity nodes on the (staggered) grid. To calculate the inter-phase momentum transfer coefficient β, for this investigation we employed the drag model of Beetstra et al. (2006), which is valid for monodisperse and polydisperse systems.

Discrete phase

The motion of droplets (in between collisions) is described by Newton's second law:

$$m_i \frac{d\mathbf{v}_i}{dt} = \sum \mathbf{F}_i = \mathbf{F}_{g,i} + \mathbf{F}_{d,i} + \mathbf{F}_{p,i} \tag{4}$$

Where m_i and $\mathbf{v}_i$ represent the mass and velocity, respectively, of the i^{th} droplets and $\sum \mathbf{F}_i$ the sum of the forces acting on that droplets. The forces consist of gravity, drag and pressure forces.

Stochastically Modified DSMC method

The Direct Simulation Monte Carlo (DSMC) method is very popular for the investigation of large numbers of particles. In the DSMC model, real particles are represented by a lower number of representative particles, and the trajectories of only these representative particles are calculated. Particle collisions are executed with a certain probability depending on the number of real particles, their velocities and their sizes. In this way, computer memory and computation time can be reduced significantly.

O'Rourke (1981) has described a version of the DSMC method in which possible collision partners are sought in rectangular cells with a fixed small time step. Du et al. (2011) have modified this approach to a model in which the path of each representative particle is updated sequentially during a large time step. The probability of particles colliding and the searching of collision partners are based on a spherical region generated from the local particle

parameters. This is our method of choice, which we will now describe in more detail.

Searching for collision partners

The region within which a droplet searches its colliding partners is called the searching scope see figure 1. After each droplet time step the searching scope range ($R_{s,i}$) is updated based on collision frequency and droplet velocities.

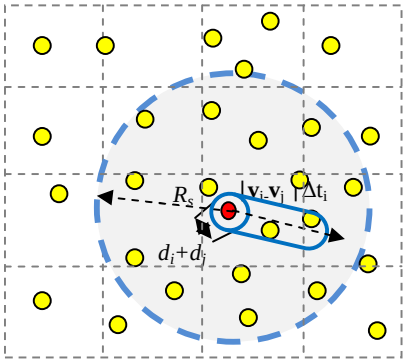

Figure 1: In DSMC a droplet (red) can collide with any of its neighboring droplets (yellow) within a certain range (dashed circle). The collision probability depends, among other things, on the relative velocity and particle size.

To update the droplet time step, we first calculate the mean free path which is analogous to the calculation of the molecular mean free path in gas dynamics. If d_i is the diameter of the moving droplet of interest (red in Figure 1) and d_j the diameter of a droplet within its searching scope (yellow), then the collision frequency of droplet i is as follows:

$$f_i = \sum_{j \in R_{s,i}} \left|\mathbf{v}_i - \mathbf{v}_j\right| \frac{\pi}{4}\left(d_i + d_j\right)^2 \frac{n_j}{\frac{4}{3}\pi\left|\max\left(R_{s,i}, R_{s,j}\right)\right|^3} \qquad (5)$$

Here $\left|\mathbf{v}_i - \mathbf{v}_j\right|$ is the value of relative velocity between the colliding droplets, $\frac{\pi}{4}\left(d_i + d_j\right)^2$ is the effective collision area, and $\frac{4}{3}\pi\left|\max\left(R_{s,i}, R_{s,j}\right)\right|^3$ is the maximum volume of the respective searching scopes. Note that we use max ($R_{s,i}$, $R_{s,j}$) because we assume that the n_j droplets represented by j are spread over a volume that scales with $R_{s,j}$. Therefore, if $R_{s,j} >> R_{s,i}$ the local number density of droplets j inside the volume set by $R_{s,i}$ is $n_j / \left(\frac{4}{3}\pi R_{s,j}\right)$. Conversely, if $R_{s,j} << R_{s,i}$ all n_j droplets are inside the volume set by $R_{s,i}$ and the average number density is $n_j / \left(\frac{4}{3}\pi R_{s,i}\right)$. The collision mean free path of the moving droplet i is calculated as:

$$L_i = \frac{\left|\mathbf{v}_i\right|}{f_i} \qquad (6)$$

During one droplet time step Δt_i, the probability of droplet collision should be less than 1. This condition is necessary to separate calculations of inter-droplet collisions from those of free droplet motion. This condition is referred to as the 'principle of uncoupling'. This condition is satisfied if the droplet time step Δt_i is calculated as follows:

$$\Delta t_i = \min\left[\frac{L_i}{3v_{i,x}}, \frac{L_i}{3v_{i,y}}, \frac{L_i}{3v_{i,z}}, \Delta t_g\right] \qquad (7)$$

Here Δt_g is the time step for updating the gas phase velocities. After each collision or gas time step, the radius of the searching scope is updated as follows:

$$R_{s,i}^{new} = \max[\left|\mathbf{v}_i\right|\Delta t_i, \left|\mathbf{v}_i - \mathbf{v}_j\right|_{\max}\Delta t_i, 2n_i^{1/3}d_i] \qquad (8)$$

Where $\left|\mathbf{v}_i - \mathbf{v}_j\right|_{\max}$ is the largest value of relative velocity between the droplets. To avoid too small a search region, $R_{s,i}$ is constrained to be at least twice the closest distance between neighbouring droplets in a dense cloud of n_i droplets of diameters d_i.

Choosing the collision partner

The collision probability between a specific pair of droplets i and j is:

$$P_{ij} = \left|\mathbf{v}_i - \mathbf{v}_j\right| \frac{\pi}{4}\left(d_i + d_j\right)^2 \frac{n_j \Delta t_i}{\frac{4}{3}\pi\left|\max\left(R_{s,i}, R_{s,j}\right)\right|^3} \qquad (9)$$

To actually choose the collision pair, with the right probability, we apply the modified Nanbu method (Tusji et al, 1998). First, a random number χ is extracted from a generator, which has a uniform distribution ranging from zero to unity. A candidate collision partner $j \in [1,.... N_i]$ is then selected from the list of neighbours using the equation

$$j = \mathrm{int}\left[\chi N_i\right] + 1 \qquad j \neq i \qquad (10)$$

Where $\mathrm{int}[x]$ is defined as the integer part of x and N_i is the total number of all representative droplets in the searching scope of droplet i. According to equation (10), an actual collision with representative droplet j is performed only if

$$\chi > \frac{j}{N_i} - P_{ij} \qquad (11)$$

From preliminary simulations, we found that it is important to add the additional condition that droplets i and j should move towards one another:

$$\left(\mathbf{v}_i - \mathbf{v}_j\right) \cdot \left(\mathbf{r}_i - \mathbf{r}_j\right) < 0 \qquad (12)$$

We have added this as a final condition for collision. Note that this reduces the real collision frequency relative to equations 6 and 9, leading to a larger mean free path. We expect this to be the same in reality. Note that this further improves the condition of uncoupling.

If all conditions are satisfied, droplet i will collide with droplet j within the droplet the time step Δt_i, and the velocities of droplets i and j are replaced with the post-collision velocities. These post-collision velocities depend on the type of collision that is taking place. In this paper we focus on droplet-droplet collisions.

Droplet-droplet collisions

The droplet-droplet collision process is one of the main events occurring during the spray drying process. Generally four different types of collisions can be distinguished, as shown in figure 2. When two droplets collide or strike each other, the gas between them is trapped and the pressure increases inside this gap. If the relative velocity of droplets is not enough to overcome the pressure force, two droplets do not intermix and simply bounce. This is referred to as bounce/rebound (a). For higher relative velocities, on the other hand, one droplet merges with another droplet directly and coalescence (b) takes place. At very high relative velocities, depending on the impact angle, the droplet breaks up again leading to reflexive (c) or stretching (d) separation, including the formation of new satellite droplets.

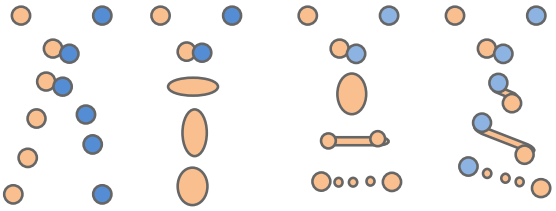

Figure 2: Diagram of collision regimes: (a) Bouncing; (b) Coalescence; (c) Reflexive separation; (d) Stretching separation

Ko et al (2005) have studied the droplet collision process in an inter-spray impingement system, both experimentally and numerically. The type of droplet collision is determined by the size ratio between the droplets, a dimensionless Weber number

$$We = \frac{\rho_d d_s \left|\mathbf{v}_{ij}\right|^2}{\sigma} \tag{13}$$

and an impact parameter

$$b = 2B / (d_s + d_l) \tag{14}$$

to decide on the outcome of a particular collision (Ashgriz and Poo, 1990; Ko et al., 2005). Here ρ_d and σ are the density and surface tension of the disperse phase, and the subscripts *s* and *l* are used for the smaller and larger droplets. Note that the Weber number is based on the smallest droplet diameter d_s. For a deterministic trajectory, the impact parameter *b* is the nondimensionalized distance *B* from the center of one droplet to that of the other in a plane perpendicular to the relative velocity vector, $\left|\mathbf{v}_{ij}\right|$, as shown in figure 3. In our simulations we do not specifically track the trajectories of all individual droplets, but only of a lower number of representative particles. The positions of these droplets are therefore not exact, but rather fuzzy. Consistent with this picture, we assume that droplets collide at a random position inside the circular (two-dimensional) collision cross-section perpendicular to the relative velocity. Because a large impact parameter b has a large probability than a smaller b, we choose b as $\sqrt{\chi}$, with χ a uniform random number between 0 and 1.

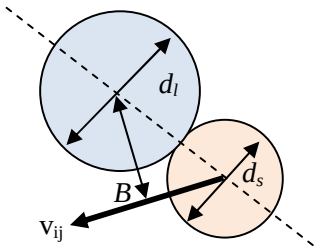

Figure 3: Collision between two droplets and definition of impact distance.

GEOMETRY AND SIMULATION CASE SET UP

In this work we study droplet dynamics in large section of a spray-dryer. We place a nozzle at 0.25m from the top wall in a rectangular channel with a cross section of 0.5m x 0.5m and a length of 1.0m, see Figure 4. For the gas dynamics we use a Cartesian grid of 20 cells in the x, y direction and 30 cells in the z direction. Prescribed pressure boundary conditions were used for the walls of the rectangular channel. A study of the effect of turbulence on droplet-droplet collision using a finer grid is planned for the future. More details of the simulation parameters are given in Table 1.

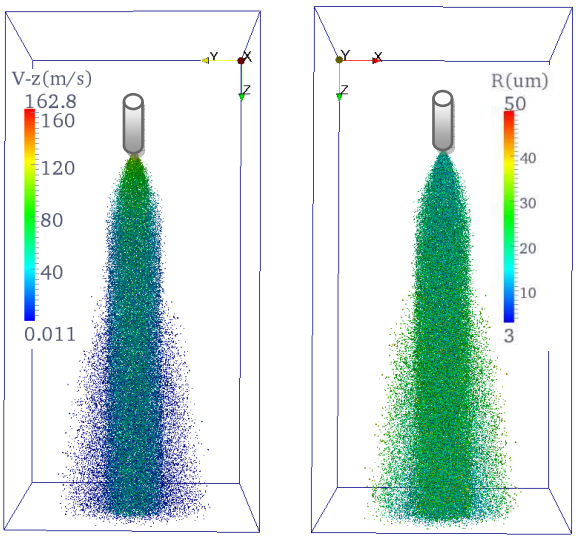

Figure 4: Schematic diagram of the geometry. Left: droplets color coded by velocity. Right: droplets color coded by radius.

Parameters	Values	Unit
Gas density (ρ_g)	1.25	kg/m^3
Viscosity of gas (μ)	1.8x10^{-5}	kg/(m s)
Density of droplets (ρ_p)	1000	kg/m^3
Surface tension of droplets (σ)	72x10^{-3}	kg/s^2
Injected droplet diameter (d_p)	40x10^{-6}	m
Nozzle diameter	4x10^{-3}	m
Spray spreading angle	73	degree
Mass flow rate	0.275	kg/s
No. droplets represented by one	1000	
Typical no. representative droplets	10^6	
Injected droplet velocity	135	m/s
Geometry dimensions (wx:dy:hz)	0.5 :0.5 :1.0	m
No. gas cells (NX:NY:NZ)	20 :20 :30	
Gas time step	2.5x10^{-6}	s
Total simulation time	10	s

Table 1: Parameters for the droplet collision dynamics

RESULTS

Validating the droplet-droplet collision type detection

We validate our implementation of the droplet-droplet collision by analyzing the collision events in a simulation of two impinging sprays of particles. The collision type depends on the size ratio between the two colliding droplets, the Weber number, and the impact parameter. As soon as a droplet crosses any of the system boundaries, it is removed from the system.

Figure 5 shows the calculated types of collisions between droplets. Each symbol represents a single collision event, characterized by a Weber number and an impact parameter. Solid lines demarcate regions of different collision type, according to the theory of Ashgriz and Poo (1990) and Ko et al. (2005), for a size ratio of 1.0. During the simulation other size ratios are also encountered, leading to a shift in these lines.

At large impact parameter or small kinetic energy (relative to the surface energy) the droplets bounce (red). For more head-on collision (smaller impact parameter) and higher kinetic energy the droplets coalesce (dark grey). At very high kinetic energy the droplets separate again, either through a stretching or reflexive mechanism, creating new satellite droplets. The higher the kinetic energy, the more satellite droplets are created. These results are in good agreement with the results of Ko et al., (2005).

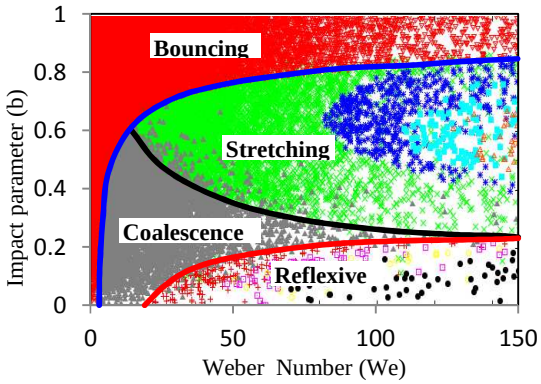

Figure 5: Calculated collision types for colliding droplets. Solid lines demarcate different regions for a size ratio of 1.0. The number of satellites are indicated by different colors. For stretching separations: green = 1, blue = 2, light blue = 3, orange = more. For reflexive separations: red = 1, pink = 2, yellow = 3, black = more.

Droplet size and velocity distribution in a single spray

We will now turn to the case of a single spray nozzle with surrounding quiescent air.

We will compare the trends of our model with the results of experiments conducted at Tetra Pak, where droplet size and velocity distributions were measured using a Phase Doppler Interferometry (PDI) system. PDI is an interferometric technique for measuring size and velocity of spherical particles. These particles can be droplets, bubbles or solid particles, as typically occur in sprays, liquid atomization and multiphase flows. A probe volume is defined by the intersection of pairs of laser beams, generating a pattern of interference by their superposition. Measurements are performed on single particles as they move through the probe volume. A portion of the optical signal generated by the scattered (refracted) light from the particles is projected onto a multiple detector system, placed at an off-axis position (approximately 30-40°). The optical signal is converted into a Doppler burst having a frequency linearly proportional to the velocity. Particle diameters are extracted from the phase shift between the Doppler signals from the detectors.

Water was sprayed into a still air environment with ambient conditions. A pressure-swirl atomizer from BETE was used in the experiments. It consists of a swirl chamber (SW06) and an orifice disc (2.31 mm). In this case driving pressure was used, 200 bar, having measured mass flow rates of 990 kg/h, respectively. A plate container having a length of 4 m and an opening cross-section of 1x1 m2 was utilized to collect and re-circulate the ejected water. In order to map as large part of the flow field as possible several measurement points were chosen across the upper part of the spray. The downstream position as well as the vertical position was varied. An axis-symmetric structure of the spray was assumed. The denseness of the spray did not allow for measurements to be conducted close to the nozzle exit. The

first reliable data was measured at a downstream position of 80 mm. After that, we measured droplets size distribution and velocity downstream of the nozzle. In each of the measurement locations the two velocity components as well as the droplet size distribution were determined.

We used the same parameter for simulation. We calculate the droplets diameter and velocity based on experimental results. In the simulations, the air flow is self-generated by the drag between the air and 40 micrometer water droplets injected at a velocity of 135 m/s. The air drag leads to a decelerating spray of droplets. The velocities of the droplets measured in the simulation model beyond 80mm have the same magnitudes (40 to 70 m/s) and directions as those observed in the experiments.

Figure 6 shows the droplet size probability distribution function in the experiments and simulations at 180 mm from the nozzle exit and 40 mm from the central axis. Note that for computational reasons we have excluded the formation of satellites with a diameter smaller than 24 micrometer. Taking this into account, the distributions are in good semi-quantitative agreement.

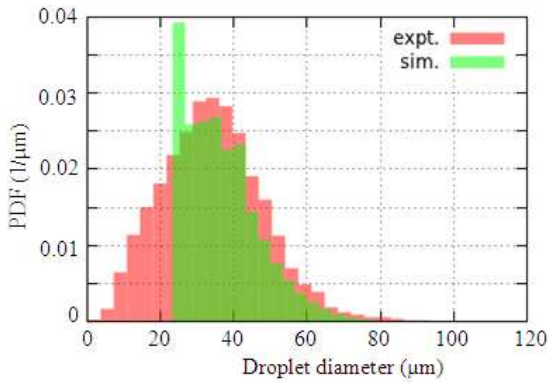

Figure 6: Droplet size probability distribution function as measured with the PDI technique (red) and in the simulation (green) at 180 mm from the nozzle exit and 40 mm from the central axis. The first peak at 24 micrometer corresponds to the smallest size of a satellite droplet allowed in our simulations.

The Sauter Mean Diameter $\langle d^3 \rangle / \langle d^2 \rangle$ was measured experimentally. Results are given in Figure 7. Generally, with increasing distance from the nozzle exit, the droplet size increases. This is caused by coalescence of droplets. It is important to note the non-trivial radial effect: with increasing distance from the central axis, the mean droplet diameter first increases, then decreases, and finally increases again.

For a qualitative comparison, we also measured the Sauter mean diameter in our simulation model. Figure 8 shows that the DSMC model reproduces all qualitative features observed in the experiments. Notably, there is a local maximum in droplet size at a finite distance from the central axis.

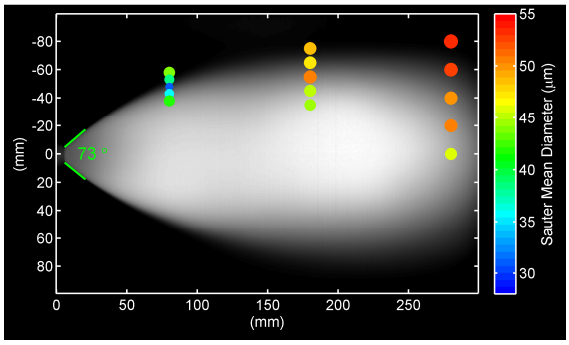

Figure 7: Sauter mean droplet diameter measured by the PDI technique at various locations in the single spray. The background image shows the time-averaged jet.

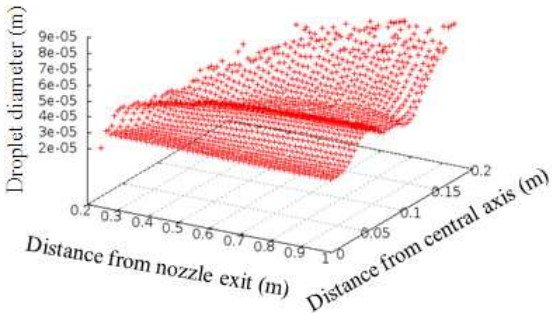

Figure 8: Sauter mean droplet diameter in the simulation model as a function of axial distance from the nozzle exit and radial distance from the central axis.

CONCLUSIONS

Spray-drying involves a complex interplay between gas turbulence and droplet and particle interaction. In this work, we implemented a stochastically modified DSMC droplet collision model, in which a very large number of droplets are represented by a smaller number of droplets and collision probabilities are calculated based on relative velocities and concentration inside a spherical region. The type of collision that occurs depends on the size ratio of the two colliding droplets, the Weber number, and the impact parameter. The predicted droplet–droplet collision events compared favorably with data from the literature.

To validate our DSMC model for droplet collisions, we studied experimentally the distribution of droplet sizes and velocities inside a single nozzle spray. We compared our simulation results at different locations inside the spray with experimental results obtained by Phase Doppler Interferometry. The results are in good semi-quantitative agreement. In future work we will use a finer grid and also study droplet-particle interactions under turbulent flow in a spray-dryer.

REFERENCES

ASHGRIZ, N., POO, J. Y., (1990),"Coalescence and Separation in Binary Collisions of Liquid Drops", *Journal of Fluid Mechanics*, 221, l83-204.

BEETSTRA, R., VAN DER HOEF, M. A., AND KUIPERS, J. A. M., (2006), "Drag force from lattice Boltzmann simulations of intermediate Reynolds number flow past mono- and bidisperse arrays of spheres", *Manuscript-AIChE J*.

BIRD, R.B., STEWART, W.E., LIGHTFOOT, E. N.,(1960), "*Transport phenomenon*", John Weily and sons, New Yark,79.

DU M., ZHAO, C., ZHAO, BIN., GUO, H., HAO. Y., (2011), "A modified DSMC method for simulating gas-particle two-phase impinging streams", *Chemical Engineering Science*, (66), 4922 -4931.

GIANFRANCESCO, A., TURCHIULI, C., DUMOULIN, E., (2008), "Powder agglomeration during the spray-drying process: measurements of air properties", *Dairy Sci. Technol*, (88), 53–64.

GOLDSCHMIDT, M.J.V., WEIJERS, G.G.C., BOEREFIJN, R., KUIPERS, J.A.M., (2003), "Discrete element modelling of fluidized bed spray granulation", *Powder Technology*, 138, 39– 45.

JIANG, Y.J., UMEMURA, A., LAW, C.K., (1992), "An experimental investigation on the collision behavior of hydrocarbon droplets", *J. Fluid Mech*. 234, 171-190.

KO, G. H., AND RYOU, H. S., (2005b), "Modeling of droplet collision-induced breakup process", *International Journal of Multiphase Flow*, (31), 723-738.

O'ROURKE, P. J., (1981), "Collective drop effect on vaporizing liquid sprays." Ph. D. thesis, *Mechanical and Aerospace Engineering*. Princeton University, USA.

TSUJI Y., TANAKA, T., YONEMURA, S.,(1998), "Cluster patterns in circulating fluidized beds predicted by numerical simulation", *Powder Technology*, 95, 254-264.

VERDURMEN, R.E.M., VERSCHUEREN, M., STRAATSMA, J., GUNSING, M., (2004), "Simulation of agglomeration in spray drying installations", *Drying Technology*, 22(6), 1403-146.

VREMAN, A.W., (2004), "An eddy- viscosity sub grid-scale model for turbulence shear flow: algebraic theory and application", Physics of fluid, 16, 3670-3681.

WOO, M.W., MUJUMDAR, A. S., DAUD W.R.W., (2010), "*Spray drying technology*", (1), 37.

